RESEARCH ARTICLE

High-Speed Sirospun Conductive Yarn for Stretchable Embedded Knitted Circuit and Self-Powered Wearable Device

Li Niu[1] · Jin Wang[1] · Kai Wang[1] · Heng Pan[2] · Gaoming Jiang[1] · Chaoyu Chen[1] · Pibo Ma[1]

Abstract

In the intelligent era, the textile technique is a high efficiency, mature and simple manufacturing solution capable of fabricating fully flexible wearable devices. However, the external circuit with its integration and comfort limitations cannot satisfy the requirements of intelligent wearable and portable devices. This study presents an industrialized production method to fabricate core–shell structure conductive yarn for direct textile use, prepared by the high-speed sirospun technique. Both integration and flexibility are significantly improved over previous works. Combining sirospun conductive yarn (SSCY) and the intarsia technique can provide the SSCY seamless and convenient embedded knitted circuit (SSCY-EKC) to form a full textile electrical element as the channel of power and signals transmission, allowing for a stable resistance change and wide strain range for meeting practical applications. SSCY based on the triboelectric nanogenerator (SSCY-TENG) can be designed as a caution carpet with attractive design and good washability for a self-powered sensor that recognizes human motions. Furthermore, intrinsic textile properties such as washability, softness, and comfort remained. With benefits such as excellent extension, fitting, and stretchability, the SSCY-EKC used herein can realize a fully flexible electrical textile with a high potential for physical detection, body gesture recognition, apparel fashion, and decoration.

Keywords Sirospun technique · Embedded knitted circuit · Intarsia technique · Stretchable · Wearable devices

Introduction

Flexible electronics with the advantages of bending, deformation, and adaptability present a wide range of potential applications in wearable devices. The rapid advancement of flexible electronics is currently altering the approach of personal healthcare [1–3], bio-motion monitors [4], and display techniques [5–7], transforming our world into an intelligent information network. Despite the fact that stretchable sensors [8–10] and flexible batteries [11–15] are connected by an external circuit for signals and power transmission, they are pasted [16–18] and sewed on the textile [19–22], reducing flexibility and comfort. Fiber-shaped electrical devices [23–26] are considered as an effective approach, improving freedom of movement, designability, and comfort, particularly textile compatibility. One-dimensional fiber structures can be used as yarn and directly integrated into two-dimensional textile via the textile process [27, 28].

Fiber-shaped conductive materials can be fabricated via diverse approaches [29], including coating [30], dipping [31], chemical plating [32], electroplating [33], chemical vapor deposition [34], and electrospinning [35], increasing the complexity of fabrication and resulting in easy exfoliation of conductive materials and poor abrasion. The conductive channel may fail over time. Furthermore, a series of textile techniques for fiber-shaped conductive yarn have been investigated, such as composite fiber spinning [36, 37] and conventional ring spinning [38]. With these technologies, the production capacity and efficiency of fiber-shaped conductive yarn have been improved. Compared to the above preparation methods, traditional textile manufacturing [13,

---

Li Niu and Jin Wang contributed equally to the work.

✉ Chaoyu Chen
chency@jiangnan.edu.cn

✉ Pibo Ma
mapibo@jiangnan.edu.cn

1 Engineering Research Center of Knitting Technology, Ministry of Education, College of Textile Science and Engineering, Jiangnan University, Wuxi 214122, China

2 State Key Laboratory of New Textile Materials and Advanced Processing Technologies, Wuhan Textile University, Wuhan 430200, China

39–44] can provide a direct and efficient way to fabricate fiber-shaped conductive yarn, which is equipped with the industrial machine and mature process, ensuring mass production, simple fabrication, low cost, high flexibility, desired human-friendliness, and high integration of fiber-shaped conductive yarn. However, a long process, poor abrasion, and a hard feel are still issues that limit wearable application.

Likewise, the pursuit of "wearable devices" includes the use of fiber-shaped conductive yarn to well integrate electronics with conventional textile. However, most electronics are still built on rigid printed circuit boards (PCBs). Despite being bendable or twistable, PCBs [45] are not a viable substitute for the real textiles in terms of maintaining intrinsic textile properties, such as flexibility, breathability, and durability. Attempts have been made to find a better way of embedding flexible electronics with a garment. Conductive patterns can be formed by screen printing [46, 47] via conductive ink coating. However, since the printing templates are not universal, the manufacturing cost is high. In addition, conductive yarns are densely sewn in the textile substrate through embroidery, making it facile to form complex and variable patterns [48]. Nevertheless, the circuit fabricated by the embroidery technique is tough, limiting the strain range and wearing comfort. Traditional textile processes, such as weaving [49] and knitting [12, 50], can be employed to integrate conductive yarn into the textile. Weaving warp and weft cannot have sufficient deformation space [51], reducing overall circuit flexibility. Knitting techniques, when compared to the woven techniques, present an appealing interactive medium for the integrated circuit and textile wearable devices due to their excellent forming, varied structures (plain [52], rib [53], double rib [54], cardigan [55]), softness, and stretchability.

Herein, the conventional sirospun technique is used to create a type of SSCY as the electronics transmission channel in this embedded-circuit construction. Using stainless steel wire as the core yarn and cotton yarn as the shell, the SSCY has been designed and manufactured to have good conductivity, high flexibility, mechanical strength, knitted adaptability, full coverage, security protection, and working durability. Fabrication parameters of SSCY have been optimized in core diameter, drafting multiples, and twist multiplier to achieve good mechanical and stable electrical properties. Due to high efficiency and mature production technology, approximately 240 m SSCY can be wrapped on the bobbin every minute. SSCY-EKC can be designed and formed by the intarsia knitting technique, which seamlessly incorporates SSCY into textile without the need of additional treatments. For the SSCY-EKC, the relative change of resistance is less than 1% under the two-dimensional tension and three-dimensional curve deformation. The full fiber knitted-based conductive channel is comfortable and tender, and it can withstand significant deformation,

long-term operation, daily washability, and wear abrasion. Two types of flexible circuit systems for light emission are applied and can still operate normally when folded and bent. Furthermore, a caution carpet is designed and prepared by using SSCY-TENG as a self-powered sensor for recognizing human motions based on the triboelectric nanogenerator (TENG). Therefore, the developed SSCY-EKC as an energy and signal transmission channel with industrial knitting, high flexibility, deformation adaptivity, working stability, and superior integration presents a promising application in real-time detection, remote healthcare, and future fashion design, and smart wearable devices.

Experimental Section

Materials

Stainless steel wires (316 L type, diameters are 0.03 mm, 0.04 mm, 0.05 mm) were purchased from Shanghai Fuxi machine, Co. Ltd., Shanghai, China. The cotton fibers (4.3 g/10 m) were brought from Weifang Honghua Textile Co., Ltd., Weifang, Shandong, China. The nylon yarn (66.7 tex) was acquired from Nantong Kejia Textile Fiber Products, Co. Ltd., Nantong, Jiangsu, China. The spandex core-spun yarns (20/70: 22.2 dtex spandex filament covered by 77.8 dtex nylon fiber; 30/70: 77.8 dtex spandex filament covered by 33.3 dtex nylon fiber; 40/70: 77.8 dtex spandex filament covered by 44.4 dtex nylon fiber) were brought from Zhuji Datang Hongnuo Fibers Co., Ltd., Zhuji, Zhejiang, China.

Design and Fabrication of SSCY

Core–shell conductive yarn is made from stainless steel wires and cotton yarns, with stainless steel wires serving as the core fiber and cotton yarns as a shell. Core fibers (stainless steel wires) are fully covered by shell fibers (cotton fibers) by the sirospun technique. First, the stainless steel wires and cotton yarns are extracted from the bobbin and pass through the guide wheel and bell, respectively. Then, two types of yarns are twisted and tied together on the spinning tube. The parameters of fiber fabrication are set, such as core fiber diameter, drawing multiple and twist. To calculate the drawing multiple, the required yarn number is divided by the actual yarn number. Finally, SSCY yarns are used for the preparation of the flexible knitted circuit.

Preparation of Flexible Knitted Circuit

In this work, all flexible knitted circuits are knitted by the knitting technique which is a mature textile process. The high-speed flat knitting machine (SWG061N2, E15, SHIMA

SEIKI, Japan) is employed to prepare a formed knitted circuit, improving the compatibility with textile. Using the intarsia technique, SSCY/spandex core-spun fiber and nylon yarn can be knitted in the designed area, respectively. A customized circuit can be knitted based on the practical application requirements.

Characterizations

The multi-functional yarn machine (CCZ-X, Wuxi Hengjiu Electrical Technology Co., LTD.) was used to prepare the SSCY. The surface morphology of yarn and textile was observed by a scanning electrons microscope (SEM) (S-4800, Hitachi, Japan). A digital multimeter (DM3068, RIGOL Technologies Co., LTD.) was used to measure resistances. The stress–strain properties were estimated by a computer-controlled electronic universal testing machine (MTS, America), and an ultrasonic cleaner (KQ-100VDV, Kunshan Ultrasonic Instruments Co., LTD.), and a Martindate Abrasimeter (YG401G, Ningbo Textile Instrument

Factory) were used to evaluate the washability and working durability of the flexible knitted circuit, respectively. The periodic contact and separation movements were applied by a commercial linear mechanical motor (LinMot E1100). The Voc, Isc, and Qsc of the BSK-TENG were measured by an electrometer (Keithley 6514).

Results and Discussion

The advantages of the textile technique, such as its high efficiency, scalable production, and diverse materials selection, have greatly promoted the development of conductive yarn and smart textile. In this study, a traditional sirospun technique is presented as a scalable fabrication of the full-coverage conductive yarn used in the embedded textile circuit, as shown in Fig. 1a. For the SSCY, stainless steel wire is chosen as the electrode, owing to its low resistance (< 10 $\Omega\,cm^{-1}$) and flexibility. Conventional cotton yarn is adopted as the shell for protecting the conductive core, which is not
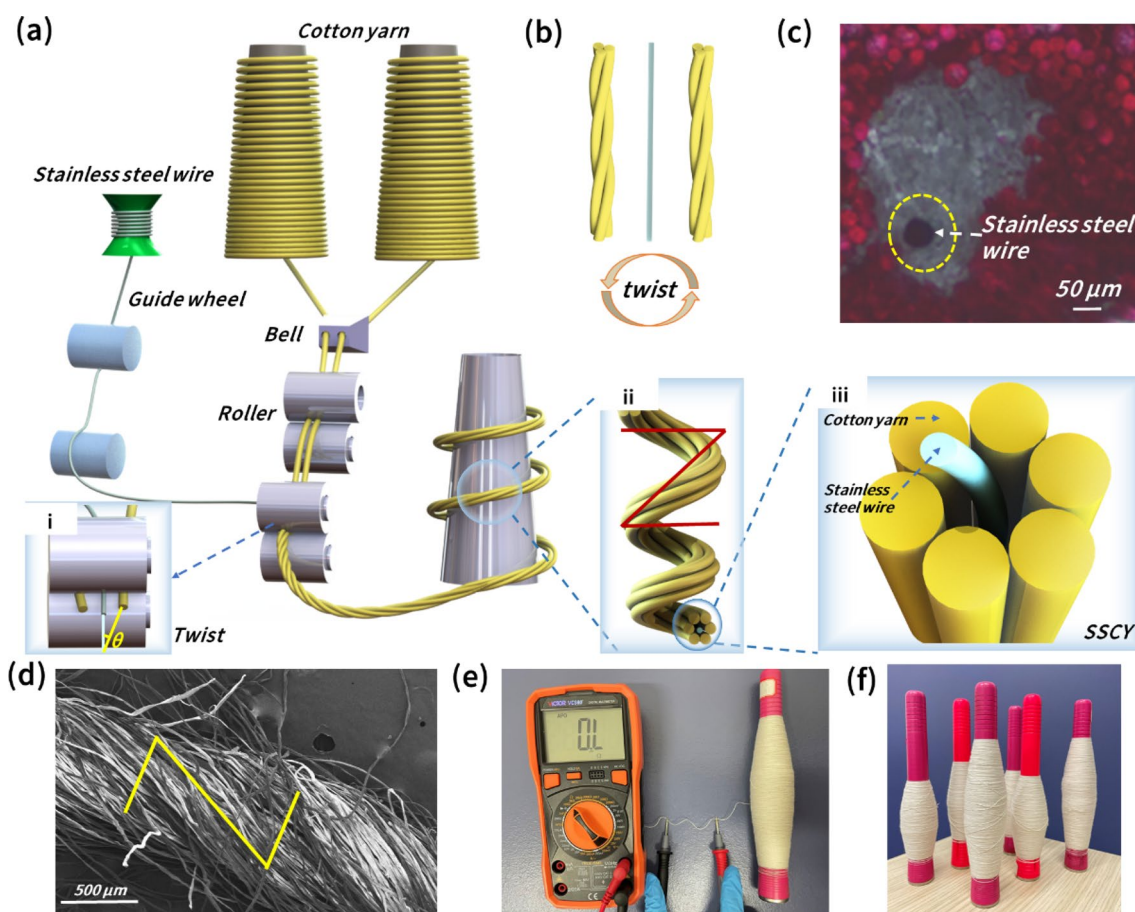

Fig. 1 Schematic illustration of the fabrication process of the SSCY. **a** Fabrication process of SSCY. (i) The twist angles. (ii) SSCY with z-twist. (iii) An enlarged view of SSCY with core–shell structure. **b** Twist cotton yarns. **c** The optical micrograph of the cross section of SSCY. **d** The SEM image of SSCY (enlarged 60 times). **e** The resistance of the surface of SSCY. **f** The large-scale production of SSCY coiled on the bobbin

only a commonly used textile material, but also has excellent wearable properties such as softness, ease of fabrication, low cost, and washability. In Fig. 1a, the spinning and continuous fabrication process of SSCY is clearly depicted as a schematic illustration. The stretchable conductive yarn is made by wrapping cotton fibers on the surface of stainless steel wire using a mature and high-speed sirospun machine. First, cotton yarn and conductive yarn are drawn from bobbins, then cotton fibers are fed into the bell and stainless steel wire is drawn by a guide wheel. Second, loose cotton fibers are drawn into the twisting triangle, forming a plied cotton yarn with weak twisting. An enlarged view of the roller is shown in Fig. 1a (i). By adjusting the twisting angle (θ), the conductive yarn can be covered by the cotton yarn with structural stability. The formed SSCY Z-twist (Fig. 1a (ii)) will be collected by a spinning tube. In Fig. 1a (iii), the shell fibers are twisted around the core conductive fibers. Then, the stainless steel wire and plied cotton yarns are twisted together (Fig. 1b). An optical micrograph of cross-sectional image and longitudinal section view of SSCY (Fig. 1c and Fig. S1) show that the bent stainless steel wire can be covered by cotton yarns and the cotton yarn on the surface of SSCY with Z-twist, as shown in Fig. 1d. The yarn surface is insulating (Fig. 1e). Considering the industrial sirospun technique, approximately 240 m of SSCY can be obtained in 1 min, confirming the ability of efficient production and promoting the commercialization of smart textile. The photograph of actual SSCY with different parameters collected on the bobbins is presented in Fig. 1f. The core–shell structure can be facile to be integrated with conductivity and flexibility, promoting the potential application of wearable devices.

The diameter of core yarn directly influences the SSCY diameter. The results show that the diameter of SSCY increases with increasing core yarn diameter (Fig. 2a). The helix appearance of SSCY is clearly shown in Fig. 2a when the core fiber is 0.03 mm, 0.04 mm, and 0.05 mm (SEMs and stress–strain curves of stainless steel wires are shown in Figs. S2 and S3), which is fabricated by a continuous and mechanical process. It is worth noting that the bare shape of stainless steel wires is twisted (Fig. 2b) due to variable speeds of fabrication motion. From the sirospun precisely static state model (Fig. 2c), the reasonable parameters of double strands spinning yarns pulling out from the front roller clips, such as yarn diameter, drawing multiple and yarn twist, can be reasonably designed for obtaining a relatively stable parameter of fabricated yarn.

The effect of three factors (yarn diameter, drawing multiple, and twist) on the bare-core length, yarn strength, and the number of turns is discussed and analyzed from Fig. 2d to Fig. 2f. Considering the structural model of SSCY (Fig. 2c), the larger the diameter (R) of SSCY, the greater is the twist angle (α). As the twist angle degree increases, so does the cohesion of a single fiber (N). The bare-core length

decreases with the increasing cohesion as the diameter of core fiber increases. It was found that the bare-core length of SSCY decreased with an increased diameter of the core fiber, verifying the structural model of SSCY. Therefore, 0.05 mm stainless steel wires as core fibers are the best candidate for the SSCY based on the shortest bare-core length. The bare-core length of SSCYs with various drawing multiples and twists is discussed. As shown in Fig. 2e–f, the same trend of an increasing bare-core length with the raised drawing multiple and twists rise. Another critical factor in successful knitting in textile manufacturing is the strength of SSCY. The little effect of drawing multiple and twisting on strength can be seen in Fig. 2e, f, which attributes to the main supporting of core yarn, not shell yarn. However, excessive twisting may hinder the stretching of SSCY. Photographs of SSCY with different drawing multiples and twists are displayed in Figs. S4 and S5. In Figs. 2f and S6, the SSCY with 410 twists has a lower strength and larger bare-core length. Figures 2g and S7 exhibit the strain–stress curve and the photograph of the testing machine is shown in Fig. S8. Stainless steel wires have a larger strain and the fracture strain ranging from 20 to 28.6%. The strain–stress curve of SSCY-0.05 mm shows two stages, wherein the first fracture occurs at 0.5% strain, as obvious in an enlarged view in Fig. 2g. This is the fracture of stainless steel wires. Then the cotton yarn is continuously stretched until it reaches a strain of 7%. Although the fracture strain of SSCY is reduced by 35%, its stress increases more than twice than that of the stainless steel wires, which is sufficient for a flexible knitted-based circuit. The stress of SSCY is obviously higher than that of the stainless steel wires owing to the combined effect of core yarn and shell yarn. The effect of the structural parameters on the elongation of SSCY is also investigated. As shown in Fig. 2h, the difference between the maximum and the minimum of elongation is less than 1%, indicating that the influence of structural parameters on elongation is small. The cyclic tensile test of SSCY is discussed in Fig. S9. It has obvious damage after ten times, due to the pullout effect of the spun fiber, as shown in Fig. S9. However, the fiber is not broken after ten times stretching.

For the requirements of the circuit, current carrying capacity, which is the ability to transfer electrons, needs to be considered. It can be expressed as relative resistance change ($\triangle R/R_0$), where $\triangle R$ is the resistance change between the initial resistance (R_0) and final resistance. As shown in Fig. 2i, the relative resistance changes of stainless steel wires show a positive linear relationship with the strain. Compared to the stainless steel wires, the relative resistance change of SSCY changes more slowly with increasing strain (Fig. 2j-l). When the structural parameter changes, resistance obviously changes with the increase in the diameter of the core yarn (Fig. 2j). The increasing resistances with different strains can reflect the change in force. As shown in Fig. 2k and l,
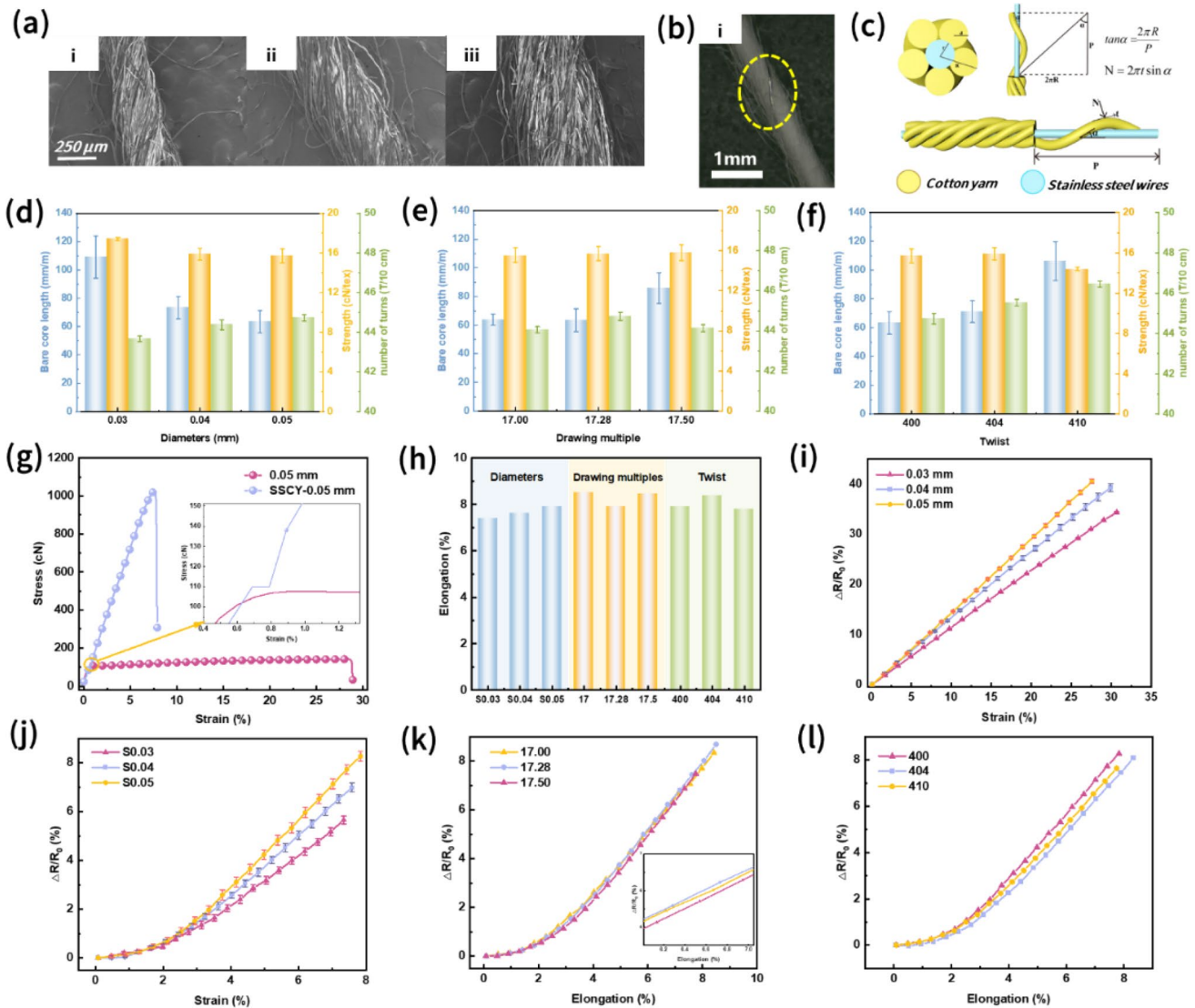
Fig. 2 Mechanical and electrical properties of SSCY. **a** The SEM of SSCY with different diameters of stainless steel wire. **b** Photograph of the shape of partial bare-core yarn. **c** Structure model of SSCY. **d**–**f** The effect of core yarn diameter, drawing multiples and twists on the bare-core length, strength, and number of turns. **g** Strain–stress curve of stainless steel wires and SSCY-0.05 mm. **h** The comparison of the effect of core yarn diameter, drawing multiples and twist on elongation. **i** Mechanical–electrical curve of stainless steel wires. **j** Mechanical–electrical curve of SSCY with different core yarn diameters. **k** Mechanical–electrical curve of SSCY with different drawing multiples. **l** Mechanical–electrical curve of SSCY with different twists

both drawing multiples and twists nearly have no influence on the conductivity. After a comprehensive consideration of bare-core length and strength, the SSCY with 0.05 mm core yarn, drawing multiple (17.28), and twist (400) is selected as the conductive yarn to fabricate the flexible knitted-based circuit for the research of integrated knitting circuit.

The chosen SSCY for a flexible circuit is integrated into the knitted textile by the intarsia knitting process (Fig. 3a), while retaining the advantages of textile properties, such as softness, stretchability, wearability, and washability. Intarsia is a knitting technique that can significantly improve the connection between two or more types of yarns, resulting

in a seamless appearance. In this study, one issue that needs to be addressed urgently is the low strain of SSCY, hindering the stretchability of SSCY-EKC. To improve elasticity, spandex core-spun yarn and SSCY are fed into the knitting needles at the same time and knitted together to fabricate the integrated flexible circuit. In addition, adding spandex core-spun yarn can improve the shortcoming of bare-core yarn, which also offers a dense and flat overlook of SSCY-EKC, as shown in Fig. S10. A linear conductive channel is embedded in the entire plain textile, forming a whole textile without extra sewing. This is a forming process that can enhance knitting efficiency and adapt to the commercialization of
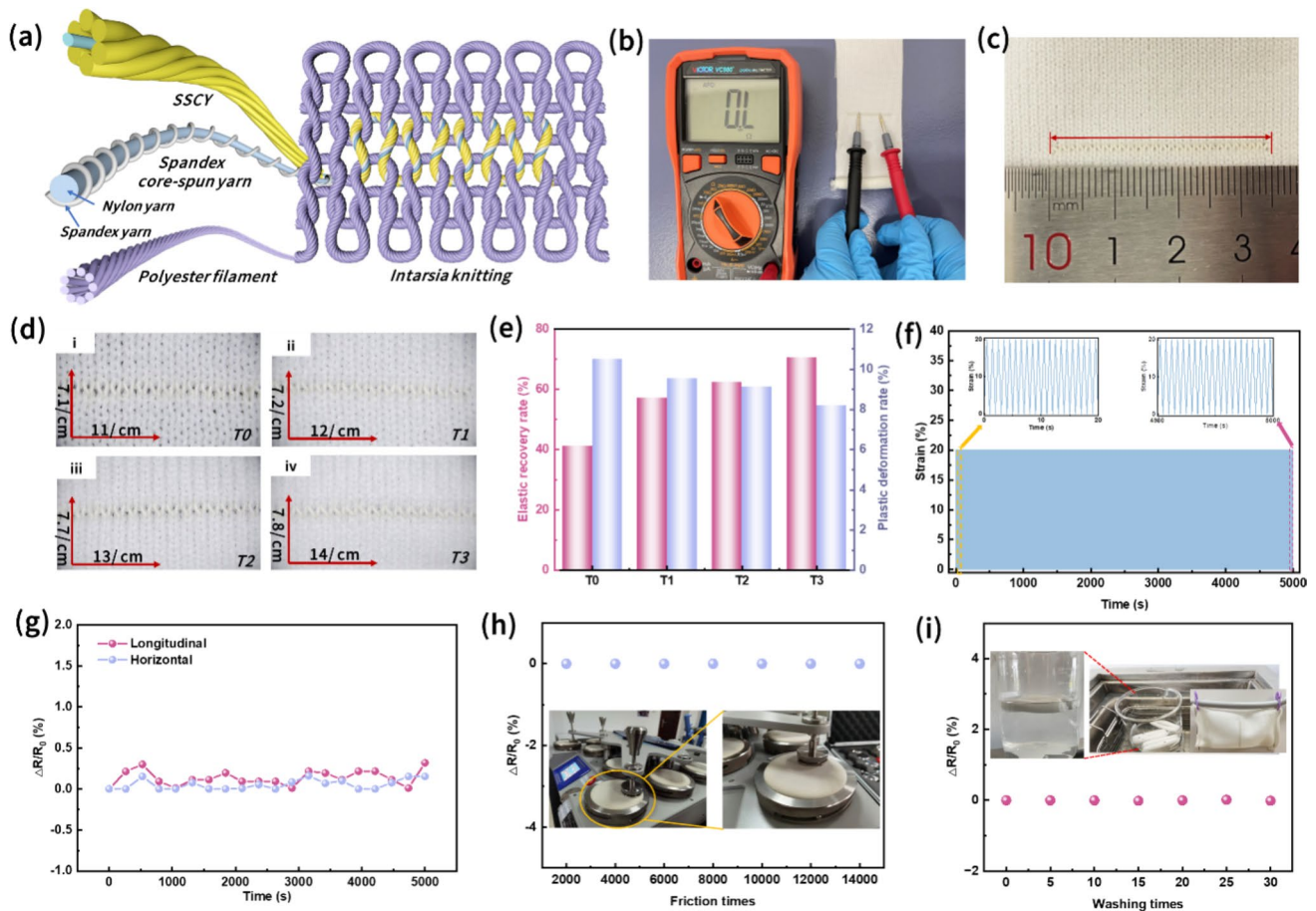
Fig. 3 The structure, mechanical, durability, and washability of the SSCY-EKC. **a** Schematic illustration of SSCY-EKC fabricated by the intarsia process. **b** The surface resistance of SSCY-EKC. **c** Photograph of the 3.5 cm SSCY-EKC integrated into the textile. **d** Photograph of SSCY-EKC with different scales of spandex core-spun yarn (T0, without spandex core-spun yarn; T1, adding 20/70 spandex core-spun yarn; T2, adding 30/70 spandex core-spun yarn; T3, adding 40/70 spandex core-spun yarn). **e** Mechanical properties of the textile with SSCY-EKC. **f** The strain stability of the SSCY-EKC is continuously tested for almost 5000 cycles. **g** The relative resistance changing durability of SSCY-EKC in the longitudinal and horizontal directions are continuously tested for almost 5000 cycles. **h** The abrasion of the SSCY-EKC. The inserted images are the testing machines and state. **i** The washability of SSCY-EKC. The inserted images are the testing machines and state

smart wearable devices. After all conductive yarn is tightly covered, cotton yarns are only exposed to the surface, ensuring the surface insulation of the flexible circuit (Fig. 3b). As shown in Fig. 3c, a 3.5 cm circuit is integrated into the textile for investigating other performances. The influence of spandex core-spun yarn on the fabrication of an SSCY-EKC should be analyzed. As illustrated in Fig. 3d, four kinds of SSCY-EKC textiles (T0, T1, T2, and T3) are fabricated with different spandex core-spun yarns. The scales of spandex core-spun fiber are 20/70, 30/70, and 40/70, consisting of nylon yarn with the same diameter, only changing diameters of spandex core-spun fiber. Course density increases with the increasing ratio of spandex fiber, as presented in Fig. 3d. The elastic recovery rates of a flexible knitted circuit are studied to explore its working durability and flexibility, as shown in Fig. 3e. T3 has the largest elastic recovery rate

(70.52%) but the lowest plastic deformation rate (8.16%). Compared to T0 without adding spandex core-spun yarn, elastic recovery rates of T1, T2, and T3 are more than 50%. Therefore, textile with spandex core-spun yarn is a better selection for fitting wearable devices. Moreover, the long-term stability of the integrated knitting circuit is discussed, which presents a stable strain value (about 20%), as shown in Fig. 3f. The details of the strain property are shown in the inserted diagram in Fig. 3f. In this study, the basic consideration is the change in relative resistance, illustrated in Fig. 3g. It turns out that the relative resistance changes can be well maintained while stretching longitudinally and horizontally. The wearing abrasion of textile is introduced in Fig. 3h. The result indicates that the relative resistance change of the SSCY-EKC has no significant decline after 14,000 friction times while still remaining 0%. Then washability is also

a necessary requirement for realizing actual wearing. The relative resistance change keeps at 0% even after 30 times washing (Fig. 3i). The excellent elasticity, stretchability, resistance changing rate, wearing abrasion, and washability of SSCY-EKC are exhibited and demonstrated to be further used in wearable devices.

As demonstrated in Fig. 4, the stability of the SSCY-EKC is discussed in terms of two-dimensional and three-dimensional deformation. The mechanical properties of SSCY-EKC textiles in vertical stretching are shown in Fig. 4a.

Comparing these results, adding spandex core-spun fiber in SSCY-EKC has an increased fracture strength and strain ability. However, the fracture strengths decrease a little in terms of textiles added spandex core-spun fiber, and T3 presents a slight decline. According to the structure of spandex core spun, the strength of SSCY is mainly derived from the nylon fiber. When continuously increasing the elasticity, the holding force between fibers decreases, resulting in a decline. However, it is also observed that fracture strain with a larger diameter of spandex fibers can have a high strain
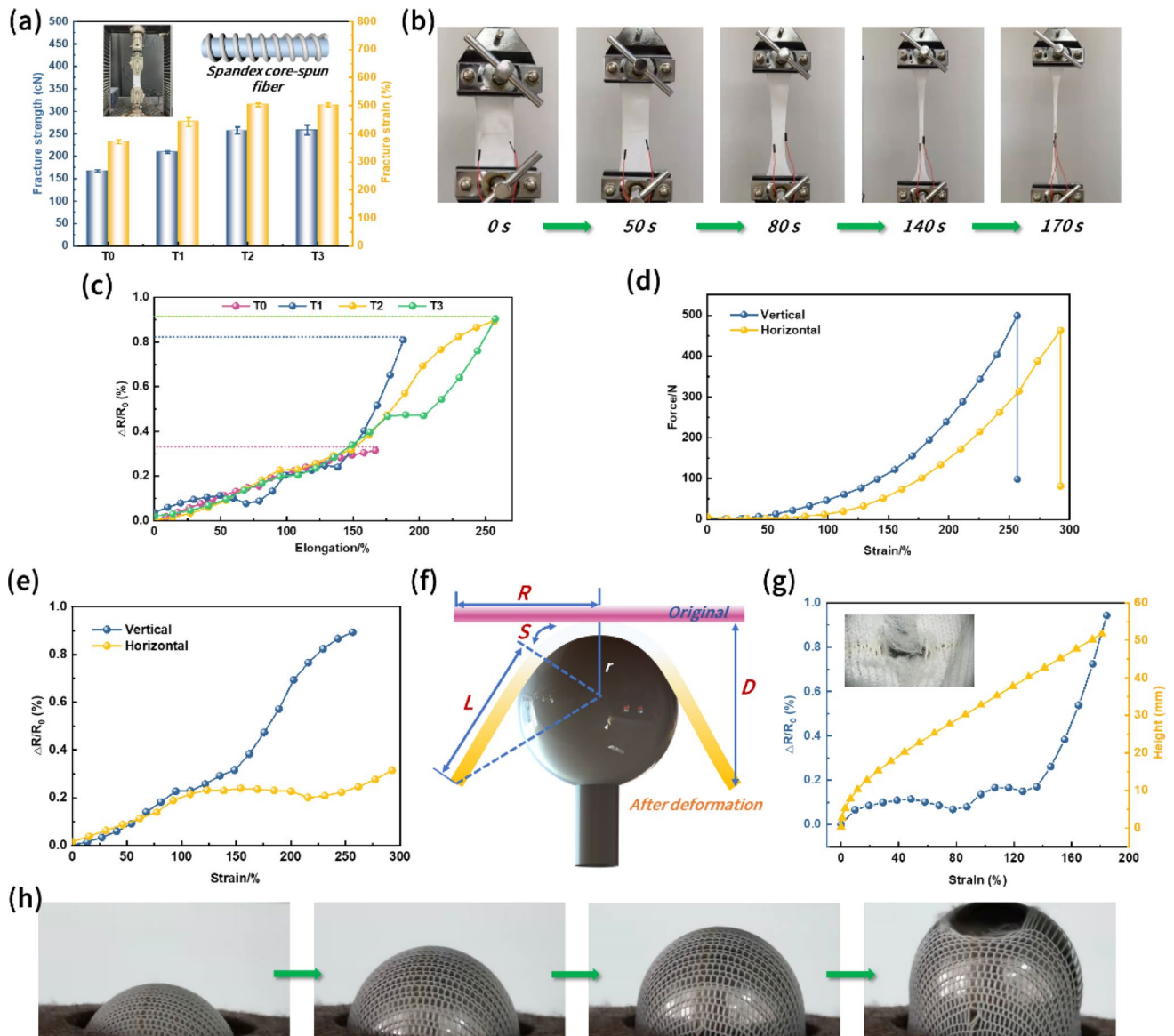

Fig. 4 Deformations of the SSCY-EKC under two-dimensional stretching and three-dimensional stretching. **a** The comparison of mechanical performances of the SSCY-EKC (T0, T1, T2, and T3), the inserted photographs are the testing status, and the schematic illustration of spandex core-spun yarn. **b** The stretching process of the longitudinal stretching for SSCY-EKC. **c** The electrical performances of the SSCY-EKC (T0, T1, T2, and T3). **d** The strain–force curve of T2. **e** The relative resistance change of T2. **f** Three-deformation model of the SSCY-EKC. **g** Resistance changing and height of T2 under three-dimensional stretching. **h** The deformation of textile under three-dimensional stretching

(257.4%). Figures 4b and S11 exhibit textile deformation under longitudinal and horizontal stretching. The break is confined to the polyester textile, not damaging the SSCY-EKC. The spandex core-spun fibers are initially stretched, and then loops are deformed under applied force. As shown in Fig. 4b, the textile is stretched in the longitudinal, but the width reduces. The effect of elasticity on the resistance properties of SSCY-EKC (Fig. 4c) have been researched. The $\triangle R/R_0$ of T0 increases linearly with increase in strain, while curves of textile-added spandex core spun are the same for strain below 175%. Over 175%, the rate of change in resistance of T2 with increasing strain is small, which is more stable as a circuit application. Hence, performances of mechanics and electricity of T2 in the latter part of this manuscript are studied. The stress–strain curve (Fig. 4d) and relative resistance change (Fig. 4e) of T2 in different directions of stretching are investigated. It is obvious that horizontal stressing shows a wider strain range (292.6%) without noticeable damage, adapting to the larger strain. Due to horizontal knitting, weft-knitting textile presents a higher stretchability in the horizontal direction. As shown in Fig. 4e, the $\triangle R/R_0$ of the vertical is nearly the same as that of the horizontal under 125%. Over 125%, the $\triangle R/R_0$ of the vertical is higher than that of the horizontal, which is affected by the loop structure change. Nevertheless, the horizontal and vertical of textile both demonstrated good stretchability and relative resistance change, which can be used as a full fiber circuit and strain sensor in future applications.

Following that, three-dimensional tensile strain can simulate the real wearing condition, so it is necessary to test it. The textile is not stretched in only one direction, rather it is a complex deformation. Figure 4f is a schematic illustration of textile surface stress and computing formula (R is the inner diameter of the bursting ring clamp; *S* is half of the arc length after the stainless steel ball contacts with the textile; *L* is the length of textile when stretching, but not in contact with the stainless steel ball; *D* is the height of the ball to break the textile), which is used to prepare a strain–height curve. The height gradually increases as the strain increases, obtaining the maximum height (51.75 mm) under 181%. As shown in Fig. 4g, the relative change in resistance increases slowly with increasing strain and then grows rapidly until the strain rises to 184.9%. Figure 4h illustrates photos of SSCY-EKC at stretched states.

SSCY-EKC provides a channel to transfer power to wearable devices to work properly. After receiving an electrified source, the textile with the pattern "KTC" can be lighted. Since the textile materials have intrinsic performances (such as flexibility and comfort), the brightness of LEDs is not affected by the textile deformation, even on bending (Fig. 5a (i)) and folding (Fig. 5a (ii)), as shown in Fig. 5a. It demonstrated the adaptability and wearability of SSCY-EKC in smart wearable devices. For the application

of smart wearable, automotive interior, and signal transferring, the flexible knitted circuit is designed and fabricated by a flat knitting machine, which is easily integrated with the ordinary knitted textile. As presented in Fig. 5b, a flexible knitted circuit with a pattern of "KTC" is seamlessly embedded in the garment through the intarsia technique and then connected by loops at the edge of the textile. The knitting process of SSCY-EKC with a "KTC" pattern is shown in Fig. S12. The captured photographs of SSCY-EKC are shown in Fig. 5c in different conditions. The lighting circuit is turned off as obvious in Fig. 5c (i), and then the circuit is turned on in the light environment (Fig. 5c (ii)) and the dark environment (Fig. 5c (iii)). It provides a potential application as a warning signal for protecting child safety in dark surroundings. In addition, optical fibers can be lighted up to serve as interior decoration of a car, as shown in Fig. 5d to Fig. 5f. The knitting process of SSCY-EKC with optical fibers is exhibited in Fig. S13. The inserted photograph of optical-fiber textile is presented in Fig. 5d. The flexible circuit can be knitted with custom patterns by the flat knitting machine. The photographs reveal the future application possibility that, even sitting in the car, we can enjoy the starry sky. As shown in Fig. 5g, the capacity of signal transmission of the purchasing piezo-resistive sensor through SSCY-EKC has been demonstrated, and the experimental value almost matches the theoretical value. The resistance of SSCY-EKC can stay stable, thus retaining the accuracy of signal transmission. In Fig. 5h, a textile with SSCY-EKC is worn on a knee to evaluate its capacity to transfer signals. SSCY-EKC changes during knee flexion and extension, inducing force changes and thus variations in the brightness of LEDs. Moreover, as different weights are placed onto the piezo-resistive sensor, signals can also be successfully and accurately transferred from SSCY-EKC, as shown in Fig. 5i. Herein, by knitting the SSCY-EKC into an apparel or textile, a full fiber power and signal transmission system can be constructed, which is important in the innovation of real smart wearable devices and smart home.

The SSCY with core–shell structure can be used as a fiber-based triboelectric nanogenerator, further integrated into the conventional textile for self-powered sensing. Figure 6 exhibits the working operation and output performances under different external conditions as a self-powered caution carpet. SSCY-TENG is knitted in a plain structure that is made up of intermeshed loops. The single-electrode mode is selected as the working operation of SSCY-TENG (Fig. 6a), with unlimited movement and can be used in different situations. The working mode is depicted in Fig. 6b. Initially, no electrical potential exists between two contacting materials under fully pressed condition. By pressing PTFE onto the textile, the surface of cotton yarn can obtain the same amount but opposite charges as the PTFE (Fig. 6b (i)). Referenced on the triboelectric series, PTFE
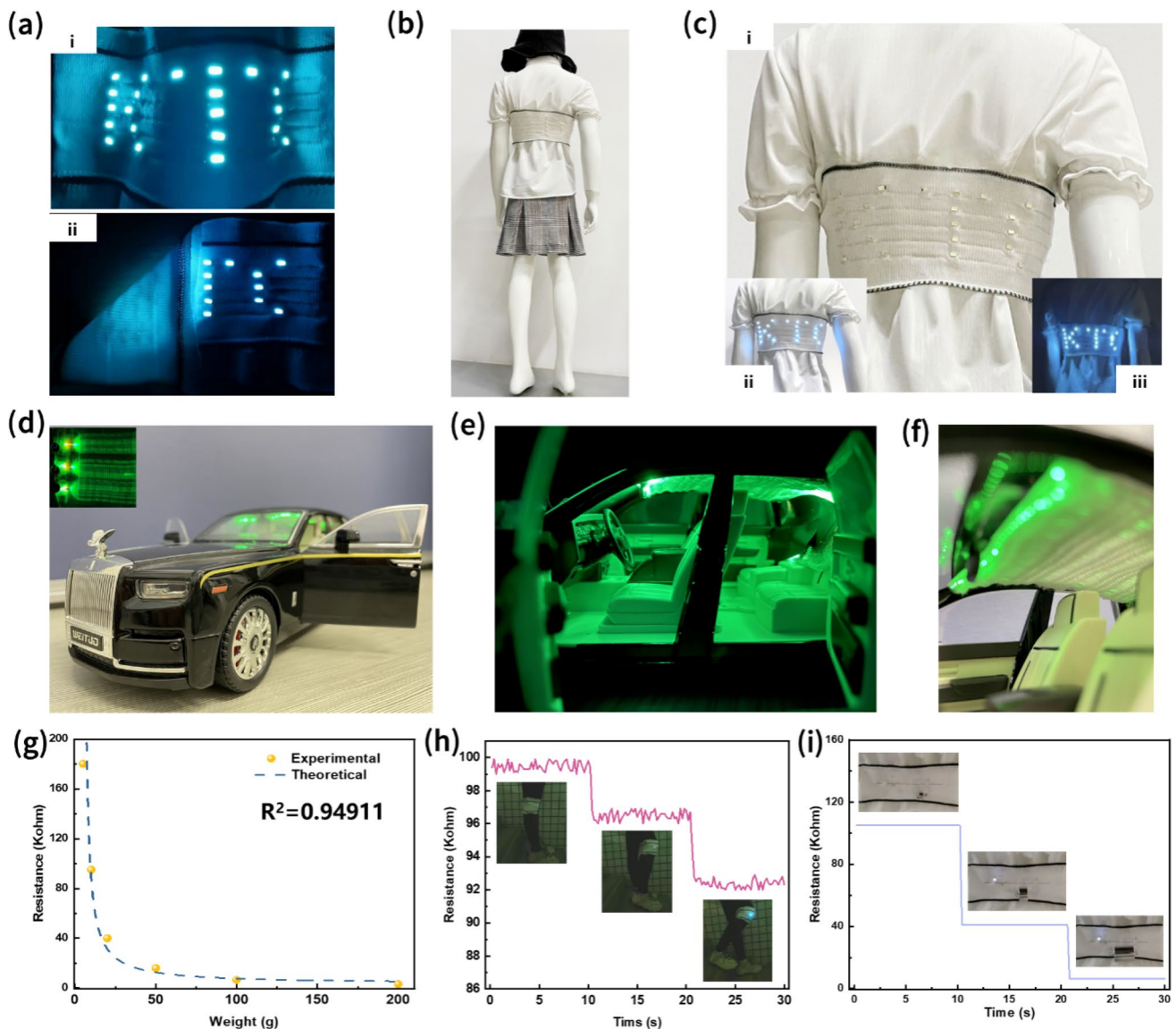
Fig. 5 Applications of the SSCY-EKC. **a** The brightness of SSCY-EKC even under bending (i) and folding (ii) status. **b** An apparel with SSCY-EKC for children's safety and protection. **c** The detailed photograph of a apparel with SSCY-EKC. (i) Unlit LEDs; (ii) lighted LEDs in a bright room; (iii) lighted LEDs in a dark room. **d–f** Optical fiber with SSCY-EKC used as the automotive interior and photographs taken from different angles. **g** Relationship between the load and resistance of the SSCY-EKC. **h** Real-time resistance of the SSCY for monitoring bending of the knee. **i** Relative resistance change of SSCY when the weight changes

has a negative triboelectric polarity which is easy to obtain electrons when contacting. As the other contact material, SSCY has been proven to be positively charged due to cotton's ability to lose more electrons than PTFE. When PTFE separates from SSCY textile, negative charges are induced in the core electrode (Fig. 6b (ii)), producing current flow from the inner electrode to the ground. As the distance between two materials increases, electrical equilibrium is achieved again and there are no moving electrons (Fig. 6b (iii)). When the PTFE moves toward the SSCY textile again, the current inversely flows from the ground to the inner electrode (Fig. 6b (iv)). Using a linear motor, the electrical outputs

can be quantitatively measured through continuous and periodic contact-separation motions and periodic electrical signals are generated. As illustrated in Fig. 6c and Fig. S14, under the test condition (the frequency is 1 Hz), output performances (open-circuit voltage (Voc), short-circuit current (Isc), and short-circuit charge quantity (Qsc)) are characterized and analyzed under varied contacting areas. The result shows that Voc, Isc, and Qsc have exhibited the increasing tendency with the increasing of contacting area increasing. The maximum Voc, Isc, and Qsc for SSCY-TENG are 7.25 V, 16.79 nA, and 0.33 nC. Furthermore, the effect of the external pressure and frequency on the electrical
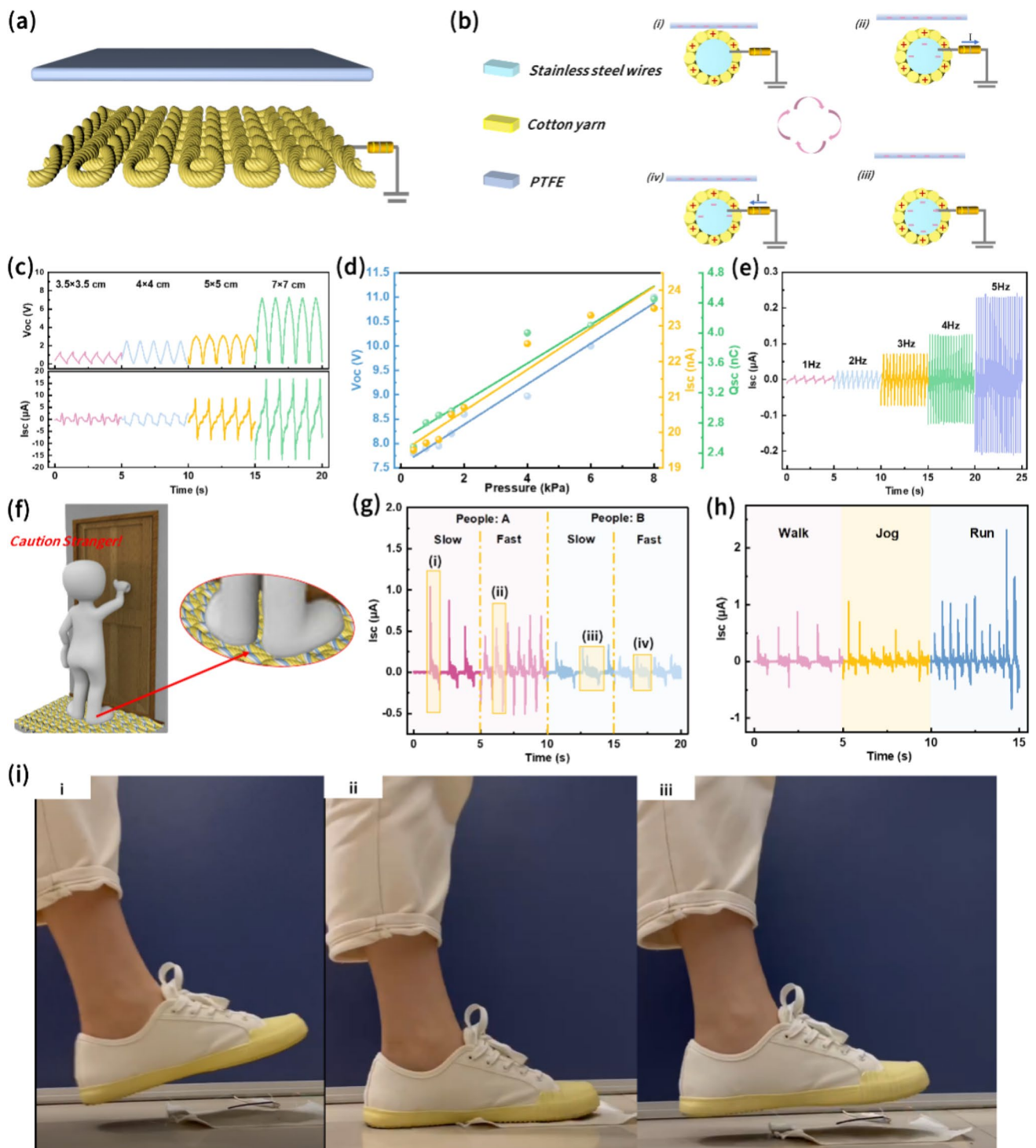
Fig. 6 Working operation and electrical output performances of SSCY-TENG as a caution carpet. **a** Schematic image of SSCY-TENG. **b** Working operation of SSCY-TENG in single-electrode mode. **c** Output performances (Voc and Isc) of SSCY-TENG with different contacting areas. **d** Output performances of SSCY-TENG with var-ied pressures. **e** Isc of the SSCY-TENG under different frequencies. **f** Schematic illustration of a caution carpet application. **g** Isc of SSCY-TENG generated by different people under different walking speeds. **h** Isc of SSCY-TENG under different statuses. **i** Photographs of the walking process

outputs was investigated. As shown in Fig. 6d and Fig. S15, it is demonstrated that the output performances (Voc, Isc, and Qsc) increase with increasing pressure from 0.8 kPa to 8 kPa, exhibiting a good linear relationship. As presented in Fig. 6e and Fig. S16, Isc of SSCY-TENG enhanced gradually with the frequency increasing from 1 to 5 Hz. Output performances with varied pressures and different frequencies can be used as a self-powered sensor for sensing force and motion frequency. When the applied frequency is 1 Hz, the peak power density of the SSCY can obtain the maximum value of 42.6 nW/ cm^2 at an external resistance of 90 MΩ (Fig. S17). The stability and reliability of Isc is indispensable for practical applications, as shown in Fig. S18. Such a continuous contact-separation motion between PTFE and SSCY textile can generate alternating electrical signals for self-powered sensing.

SSCY-TENG with good output performances can be used as a self-powered caution carpet (Fig. 6f), while maintaining the softness and washability of conventional textile. Everyone has their own walking habits (including force of landing, step frequency, etc.); therefore, two parameters may be used as sensing signals. Furthermore, the electrical outputs of SSCY-TENG change regularly as the test parameters change in different forces and frequencies. Either forces or frequencies can be used to recognize different people. So a caution carpet is designed and used for intelligent protection. As shown in Fig. 6g and h, different people and movements with various walking frequencies can be distinguished by a short-circuit current. Comparing the test results, the Isc generated by walking on the SSCY-TENG by person A with a large body weight is larger than that of person B with a small body weight. In addition, with different moving frequencies, slow walking exhibits much more time between two peaks than fast walking, such as (i) > (ii), (iii) > (iv) (in Fig. S19). The whole walking action can be seen in Fig. 6i. Based on the influence of frequency on the Isc, the result shows obviously varied output performances under walking, jogging, and running. The SSCY-TENG carpet presents a potential application for real-time movement detection, and human–computer interaction for smart wearable devices and intelligent protection.

Conclusion

In summary, an SSCY with a core–shell structure composed of stainless steel wires and cotton yarn is fabricated by the traditional sirospun technique. Based on the advantages of high efficiency and mature technique, approximately 240 m SSCY can be made per minute, which accelerates the marketization of conductive materials and smart wearable devices. To optimize the bare-core length and strength, parameters of SSCY designed in 0.05 mm core yarn,

drawing multiple (17.28) and twist (400), is selected as the conductive yarn to fabricate the SSCY-EKC. Then, SSCY is easily embedded into the knitted textile by the intarsia technique, and a highly SSCY-EKC is prepared and systematically researched. Adding spandex core-spun yarn enhances the stretchability of SSCY-EKC, while maintaining a stable resistance change. This SSCY can not only be used for power transmission (such as a warning garment, automotive interior), but also as a self-powered caution carpet for movement detection. This work provides an industrial production of novel conductive yarn with high stretchability, comfortability, washability, and abrasion resistance, which have a great progress and innovation in full flexible sensing system.

Declarations

Conflict of interest The authors declare no competing financial interests.

References

1. Wei PQ, Yang X, Cao ZM, Guo XL, Jiang HL, Chen Y, Morikado M, Qiu XB, Yu D. Flexible and stretchable electronic skin with high durability and shock resistance via embedded 3D printing technology for human activity monitoring and personal healthcare. *Adv Mater Technol* **2019**;*4*:1900315.
2. Liu Y, Pharr M, Salvatore GA. Lab-on-Skin: a review of flexible and stretchable electronics for wearable health monitoring. *ACS Nano* **2017**;*11*:9614.
3. Chen J, Li L, Zhu Z, Luo Z, Tang W, Wang L, Li H. Bioinspired design of highly sensitive flexible tactile sensors for wearable healthcare monitoring. *Mater Today Chem* **2022**;*23*:100718.
4. Gao YY, Li Z, Xu BG, Li MQ, Jiang CHZ, Guan XY, Yang YJ. Scalable core–spun coating yarn-based triboelectric nanogenerators with hierarchical structure for wearable energy harvesting and sensing via continuous manufacturing. *Nano Energy* **2022**;*91*:106672.
5. Shi X, Zuo Y, Zhai P, Shen J, Yang Y, Gao Z, Liao M, Wu J, Wang J, Xu X, Tong Q, Zhang B, Wang B, Sun X, Zhang L, Pei Q, Jin D, Chen P, Peng H. Large-area display textiles integrated with functional systems. *Nature* **2021**;*591*:240.
6. Koo JH, Kim DC, Shim HJ, Kim TH, Kim DH. Flexible and stretchable smart display: materials, fabrication, device design, and system integration. *Adv Funct Mater* **2018**;*28*:1801834.
7. Wang Y, Ren J, Ye C, Pei Y, Ling S. Thermochromic silks for temperature management and dynamic textile displays. *Nano-Micro Lett* **2021**;*13*:1.
8. Yang Y, Deng ZD. Stretchable sensors for environmental monitoring. *Appl Phys Rev* **2019**;*6*:011309.

9. Wu ZX, Yang X, Wu J. Conductive hydrogel-and organohy-drogel-based stretchable sensors. *ACS Appl Mater Interfaces* **2021**;*13*:2128.

10. Zhang YZ, Lin ZK, Huang XP, You XJ, Ye JH, Wu HB. A Large-area, stretchable, textile-based tactile sensor. *Adv Mater Technol* **2020**;*5*:1901060.

11. Wang DH, Sun JF, Xue Q, Li Q, Guo Y, Zhao YW, Chen Z, Huang ZD, Yang Q, Liang GJ. A universal method towards conductive textile for flexible batteries with superior softness. *Energy Stor Mater* **2021**;*36*:272.

12. Dong K, Wang YC, Deng J, Dai Y, Zhang SL, Zou H, Gu B, Sun B, Wang ZL. A highly stretchable and washable all-yarn-based self-charging knitting power textile composed of fiber triboelectric nanogenerators and supercapacitors. *ACS Nano* **2017**;*11*:9490.

13. Wen Z, Yeh MH, Guo HY, Wang J, Zi YL, Xu WD, Deng JN, Zhu L, Wang X, Hu CG. Self-powered textile for wearable electronics by hybridizing fiber-shaped nanogenerators, solar cells, and supercapacitors. *Sci Adv* **2016**;*2*:e1600097.

14. Liao M, Ye L, Zhang Y, Chen TQ, Peng HS. The recent advance in fiber-shaped energy storage devices. *Adv Electron Mater* **2019**;*5*:1800456.

15. Ye C, Dong S, Ren J, Ling S. Ultrastable and high-performance silk energy harvesting textiles. *Nano-Micro Lett* **2020**;*12*:1.

16. Soroudi A, Hernández N, Wipenmyr J, Nierstrasz V. Surface modification of textile electrodes to improve electrocardiography signals in wearable smart garment. *J Mater Sci Electron* **2019**;*30*:16666.

17. Nasiri S, Khosravani MR. Progress and challenges in fabrication of wearable sensors for health monitoring. *Sens Actuators A* **2020**;*312*:112105.

18. Kuzubasoglu BA, Bahadir SK. Flexible temperature sensors: a review. *Sens Actuators A* **2020**;*315*:112282.

19. García Patiño A, Khoshnam M, Menon C. Wearable device to monitor back movements using an inductive textile sensor. *Sensors* **2020**;*20*:905.

20. Samad YA, Komatsu K, Yamashita D, Li Y, Zheng L, Alhassan SM, Nakano Y, Liao K. From sewing thread to sensor: Nylon® fiber strain and pressure sensors. *Sens. Actuator B* **2017**;*240*:1083.

21. Shin Y-E, Lee J-E, Park Y, Hwang S-H, Chae HG, Ko H. Sewing machine stitching of polyvinylidene fluoride fibers: programmable textile patterns for wearable triboelectric sensors. *J Mater Chem A* **2018**;*6*:22879.

22. Honda S, Zhu Q, Satoh S, Arie T, Akita S, Takei K. Textile-based flexible tactile force sensor sheet. *Adv Funct Mater* **2019**;*29*:1807957.

23. De Rossi D. Electronic textiles: a logical step. *Nat Mater* **2007**;*6*:328.

24. Jinno H, Fukuda K, Xu XM, Park S, Suzuki Y, Koizumi M, Yokota T, Osaka I, Takimiya K, Someya T. Stretchable and waterproof elastomer-coated organic photovoltaics for washable electronic textile applications. *Nat Energy* **2017**;*2*:780.

25. Zhang NN, Huang F, Zhao SL, Lv XH, Zhou YH, Xiang SW, Xu SM, Li YZ, Chen GR, Tao CY. Photo-rechargeable fabrics as sustainable and robust power sources for wearable bioelectronics. *Matter* **2020**;*2*:1260.

26. Lee J, Kwon H, Seo J, Shin S, Koo JH, Pang C, Son S, Kim JH, Jang YH, Kim DE. Conductive fiber-based ultrasensitive textile pressure sensor for wearable electronics. *Adv Mater* **2015**;*27*:2433.

27. Shi QW, Sun JQ, Hou CY, Li YG, Zhang QH, Wang HZ. Advanced functional fiber and smart textile. *Adv Fiber Mater* **2019**;*1*:3.

28. Weng W, Yang JJ, Zhang Y, Li YX, Yang SY, Zhu LP, Zhu MF. A route toward smart system integration: from fiber design to device construction. *Adv Mater* **2020**;*32*:1902301.

29. Li X, Chen S, Peng Y, Zheng Z, Li J, Zhong F. Materials, preparation strategies, and wearable sensor applications of conductive fibers: a review. *Sensors* **2022**;*22*:3028.

30. Yang M, Pan J, Xu A, Luo L, Cheng D, Cai G, Wang J, Tang B, Wang X. Conductive cotton fabrics for motion sensing and heating applications. *Polymers (Basel)* **2018**;*10*:568.

31. Fakharuddin A, Li H, Di Giacomo F, Zhang T, Gasparini N, Elezzabi AY, Mohanty A, Ramadoss A, Ling J, Soultati A. Fiber-shaped electronic devices. *Adv Energy Mater* **2021**;*11*:2101443.

32. Lu L-F, Cao X-J, Qi S-H. Properties investigation on electrically conductive adhesives based on acrylate resin filled with silver microsheets and silver plating carbon fibers. *J Adhes Sci Technol* **2017**;*31*:1747.

33. Munirathinam K, Park J, Jeong Y-J, Lee D-W. Galinstan-based flexible microfluidic device for wireless human-sensor applications. *Sens Actuators B* **2020**;*315*:112344.

34. Tran TQ, Lee JKY, Chinnappan A, Loc NH, Tran LT, Ji D, Jayathilaka W, Kumar VV, Ramakrishna S. High-performance carbon fiber/gold/copper composite wires for lightweight electrical cables. *J Mater Sci Technol* **2020**;*42*:46.

35. Xue LL, Fan W, Yu Y, Dong K, Liu CK, Sun YL, Zhang C, Chen WC, Lei RX, Rong K. A novel strategy to fabricate core-sheath structure piezoelectric yarns for wearable energy harvesters. *Adv Fiber Mater* **2021**;*3*:239.

36. Seyedin S, Zhang P, Naebe M, Qin S, Chen J, Wang X, Razal JM. Textile strain sensors: a review of the fabrication technologies, performance evaluation and applications. *Mater Horizons* **2019**;*6*:219.

37. Seyedin S, Razal JM, Innis PC, Jeiranikhameneh A, Beirne S, Wallace GG. Knitted srain sensor textiles of highly conductive all-polymeric fibers. *ACS Appl Mater Interfaces* **2015**;*7*:21150.

38. Özen Ö, Yilmaz D, Yapici K. A novel method for the production of conductive ring spun yarn. *Cellulose* **2022**;*29*:4767.

39. Dong K, Wu Z, Deng J, Wang AC, Zou HY, Chen C, Hu D, Gu B, Sun B, Wang ZL. A stretchable yarn embedded triboelectric nanogenerator as electronic skin for biomechanical energy harvesting and multifunctional pressure sensing. *Adv Mater* **2018**;*30*:1804944.

40. Chen CY, Guo HY, Chen LJ, Wang YC, Pu XJ, Yu WD, Wang FM, Du ZQ, Wang ZL. Direct current fabric triboelectric nanogenerator for biomotion energy harvesting. *ACS Nano* **2020**;*14*:4585.

41. Niu L, Miao X, Jiang G, Wan A, Li Y, Liu Q. Biomechanical energy harvest based on textiles used in self-powering clothing. *J Eng Fibers Fabr* **2020**;*15*:1558925020967352.

42. Dong K, Peng X, An J, Wang AC, Luo JJ, Sun BZ, Wang J, Wang ZL. Shape adaptable and highly resilient 3D braided triboelectric nanogenerators as e-textiles for power and sensing. *Nat Commun* **2020**;*11*:1.

43. Ning C, Cheng RW, Jiang Y, Sheng FF, Yi J, Shen S, Zhang Y, Peng X, Dong K, Wang ZL. Helical fiber strain sensors based on triboelectric nanogenerators for self-powered human respiratory monitoring. *ACS Nano* **2022**;*16*:2811.

44. Niu L, Peng X, Chen LJ, Liu Q, Wang TR, Dong K, Pan H, Cong HL, Liu GL, Jiang GM. Industrial production of bionic scales knitting fabric-based triboelectric nanogenerator for outdoor rescue and human protection. *Nano Energy* **2022**;*97*:107168.

45. Alwaidh A, Sharp M, French P. Laser processing of rigid and flexible PCBs. *Opt Laser Eng* **2014**;*58*:109.

46. Brooke R, Wijeratne K, Hübscher K, Belaineh D, Andersson EP. Combining vapor phase polymerization and screen printing

for printed electronics on flexible substrates. *Adv Mater Technol* **2022**;*7*:2101665.

47. Song ZW, Yin JH, Wang ZH, Lu CY, Yang Z, Zhao ZH, Lin ZN, Wang JY, Wu CS, Cheng J. A flexible triboelectric tactile sensor for simultaneous material and texture recognition. *Nano Energy* **2022**;*93*:106798.

48. de Mulatier S, Nasreldin M, Delattre R, Ramuz M, Djenizian T. Electronic circuits integration in textiles for data processing in wearable technologies. *Adv Mater Technol* **2018**;*3*:1700320.

49. Yu A, Pu X, Wen R, Liu M, Zhou T, Zhang K, Zhang Y, Zhai J, Hu W, Wang ZL. Core–shell-yarn-based triboelectric nanogenerator textiles as power cloths. *ACS Nano* **2017**;*11*:12764.

50. Kwak S, Kim H, Seung W, Kim J, Hinchet R, Kim S. Fully stretchable textile triboelectric nanogenerator with knitted fabric structures. *ACS Nano* **2017**;*11*:10733.

51. Dong K, Hu YF, Yang J, Kim S-W, Hu WG, Wang ZL. Smart textile triboelectric nanogenerators: current status and perspectives. *MRS Bull* **2021**;*46*:512.

52. Huang T, Zhang J, Yu B, Yu H, Long H, Wang H, Zhang Q, Zhu M. Fabric texture design for boosting the performance of a knitted washable textile triboelectric nanogenerator as wearable power. *Nano Energy* **2019**;*58*:375.

53. Niu L, Miao X, Li Y, Xie X, Wen Z, Jiang G. Surface morphology analysis of knit structure-based triboelectric nanogenerator for enhancing the transfer charge. *Nanoscale Res Lett* **2020**;*15*:1.

54. Chen C, Chen L, Wu Z, Guo H, Yu W, Du Z, Wang Z. 3D double-faced interlock fabric triboelectric nanogenerator for bio-motion energy harvesting and as self-powered stretching and 3D tactile sensors. *Mater Today* **2020**;*32*:84.

55. Fan W, He Q, Meng K, Tan X, Zhou Z, Zhang G, Yang J, Wang Z. Machine-knitted washable sensor array textile for precise epidermal physiological signal monitoring. *Sci Adv* **2020**;*6*:eaay2840.

Publisher's Note Springer Nature remains neutral with regard to jurisdictional claims in published maps and institutional affiliations.

Li Niu received her M.S. degree in School of Textile Science and Engineering, Tiangong University in 2018. Now pursuing her Ph.D. degree at Jiangnan University. Her research interests focus on knitting technique, fiber/textile-based triboelectric nanogenerator, self-powered wearable sensors, and smart electronic textile.

Jin Wang received her M.S degree in textile engineering from Jiangnan University in 2022 and her B.S. degrees in textile engineering from Anhui Polytechnic University in 2019. Her research interests focus on smart textile, flexible sensors, and wearable devices.

Kai Wang received her B.S. degrees in textile engineering from Jiangnan University in 2021. Currently, she is pursuing her M.S. degree at Jiangnan University. Her research interests include high-performance textile-based triboelectric nanogenerators, and wearable devices.

Heng Pan received M.S. degree (2018) in textile science and engineering from Wuhan Textile University. Now is a senior research associate of State Key Laboratory of New Textile Materials and Advanced Processing Technologies at Wuhan Textile University. He has participated in the lunar flag project and the design of high-performance textile structure reinforcement materials. His current research interest is structural design of textile materials for supercapacitors.

Prof. Gaoming Jiang is the director in Engineering Research Center of Knitting Technology, Ministry of Education, College of Textile Science and Engineering, Jiangnan University. He received P.H. degree (2007) in Textile Engineering from Donghua University. His research interests include knitting technique, knitting simulation, smart knitting machine.

Chaoyu Chen received his Ph.D. degree in textile science and engineering from Donghua university in 2020. During 2017–2019, he was supported by the program of China Scholarship Council (CSC) as a joint Ph.D. student in Georgia Institute of Technology (GT). He has joined in Engineering Research Center of Knitting Technology, Ministry of Education, College of Textile Science and Engineering, Jiangnan University as an assistant professor since 2021. His main research interests focus on fiber/textile based wearable electronic devices, biomechanical energy harvesting, self-powered textile sensors.

Pibo Ma received his Ph.D. degree in from Donghua university in 2012. Now he is a professor of Textile Science and Engineering at Jiangnan University. During 2011–2012, he was supported by the program of China Scholarship Council (CSC) as a joint Ph.D. student in Georgia Institute of Technology (GT). His research interests focus on the design and performance research of industrial textile, textile structural flexible materials, and smart textile material.